HPV-negative Squamous Cell Carcinomas of the Cervix With Special Focus on Intraepithelial Precursor Lesions

Sigrid Regauer, MD, Olaf Reich, MD,† and Karl Kashofer, PhD**

Abstract: Recently, the World Health Organization (WHO) recognized human papilloma virus (HPV)-independent invasive cervical squamous cell carcinoma (SCC) without recognizing the existence of precursor lesions. This is a detailed characterization of 3 preinvasive lesions and 6 invasive SCC negative for HPV-DNA (32 genotypes), HPV-mRNA (14 genotypes) and genomic HPV sequencing. We evaluated histologic features, expression of $p16^{ink4a}$, p53, CK7, and CK17, aberrations in 50 cancer genes and chromosomal copy number variations. HPV-negative preinvasive lesions were extensive basaloid or highly differentiated keratinizing intraepithelial proliferations of 3 to 20 cell layers thickness, partly with prominent cervical gland involvement. Overall, 2/3 intraepithelial lesions and the in situ component of 1/6 SCC showed $p16^{ink4a}$ block staining, while 1/6 in situ component revealed heterogenous $p16^{ink4a}$ staining. All invasive components of keratinizing SCC were $p16^{ink4a}$-negative. Preinvasive and invasive SCC showed inconsistent CK7 and CK17 staining. Nuclear p53 overexpression was restricted to the *TP53* gene mutated SCC. The highly vascularized peritumoral stroma showed a dense inflammatory infiltrate including plasma cells and intratumoral and peritumoral eosinophilic granulocytes. Inconsistent somatic gene mutations (PIK3CA, STK11, TP53, SMARC2B, and GNAS) occurred predominantly in nonhotspot locations at low mutational frequency in 3/6 SCC. Consistent aberrations included the pathogenic (angiogenic) germline polymorphism Q472H in the KDR gene (7/9 patients), and chromosome 3q gains (4/9 patients). In conclusion, HPV-negative intraepithelial cervical precancerous lesions exist, either as highly differentiated keratinized intraepithelial proliferations reminiscent of differentiated vulvar intraepithelial neoplasia, or undifferentiated basaloid intraepithelial lesions with occasional $p16^{ink4a}$ block staining resembling high-grade squamous intraepithelial lesion. Gains of chromosome 3q, angiogenic germline variants the inflammatory infiltrate may contribute to progression of HPV-negative cervical carcinogenesis.

From the *Diagnostic and Research Institute of Pathology; and †Department of Obstetrics and Gynecology, Medical University Graz, Graz, Austria.

S.R. and K.K. contributed equally.

Conflicts of Interest and Source of Funding: The authors have disclosed that they have no significant relationships with, or financial interest in, any commercial companies pertaining to this article.

Correspondence: Sigrid Regauer, MD, Diagnostic and Research Institute of Pathology, Medical University Graz, MedCampus Graz, Neue Stiftingtalstrasse 6, Graz 8010, Austria (e-mail: sigrid.regauer@medunigraz.at).

Key Words: HPV-negative cervical carcinogenesis, HPV gene sequencing, HPV-DNA test, cancer hotspot panel, genetic aberrations, germline polymorphisms, chromosomal copy number variations, $p16^{ink4a}$ overexpression

(*Am J Surg Pathol* 2021;00:000–000)

For decades transforming human papilloma virus (HPV) infections were considered the causal factor for cervical squamous cell carcinomas (SCC).[1,2] HPV high-grade E6 and E7 oncogene-mediated cell cycle disruptions lead to development of *high-grade squamous intraepithelial lesion (HSIL)* with cytoplasmic accumulation/overexpression of $p16^{ink4a}$. Progression to invasive and metastatic cervical SCC is enhanced by genetic abberations, most importantly activating PIK3CA (driver) gene mutations.[3,4] For the first time in 2020, the existence of HPV-independent invasive cervical cancers was recognized by the World Health Organization (WHO).[5] Data on this entity are scarce, even in specialized centers with 3 invasive SCC reported in a Swedish patient cohort[6] and 12 invasive SCC in a Catalonian population.[7] Isolated HPV-negative precursor lesions, however, were not identified in these studies, nor in the US-based Athena Trial or another large study of over 500 patients.[8,9] The WHO therefore did not recognize precursor lesions for HPV-negative SCC. Some authors even doubt the existence of intraepithelial precursor lesions. We reported recently—without further detailed documentation—preinvasive lesions negative with 3 different HPV tests in a series of 474 cone specimens.[10] In the meantime, we identified 3 cervical precursor lesions without associated invasive SCC and 6 additional invasive SCC which are negative for HPV-DNA of 32 HPV genotypes and mRNA of 14 HPV high-risk genotypes. Here, we report for the first time detailed histomorphologic and immunohistochemical characteristics of HPV-negative precursor and invasive lesions including analysis of actionable somatic gene mutations in hotspot regions of 50 cancer-related genes and whole-genome chromosomal copy number variations. Special focus was placed on characterization of the preinvasive in situ components of invasive SCC.

MATERIALS AND METHODS

HPV Testing

Three different HPV tests were performed for each patient. Pretreatment liquid-based cytology specimens

(Roche HPV assay; Roche Molecular Systems, Pleasanton, CA) were subjected to the Aptima HPV Assay (which detects E6/E7 mRNA; Hologic) and the Cobas HPV test (Roche HPV assay, which detects HPV-DNA; Roche Molecular Systems). These tests detect 14 high-risk HPV types (HPV 16, 18, 31, 33, 35, 39, 45, 51, 52, 56, 58, 59, 66, and 68). After surgical treatment, HPV genotyping was performed on microdissected formalin-fixed and paraffin-embedded lesional tissue. The CHIPRON HPV3.5LCD-array (CHIPRON GmbH, Berlin, Germany) detects DNA of 32 HPV subtypes. These include HPV high-risk subtypes 16, 18, 31, 33, 35, 39, 45, 51, 52, 56, 58, and 59; HPV low-risk subtypes 6 and 11; probably carcinogenic HPV subtype 68; possibly carcinogenic HPV subtypes 26, 53, 66, 67, 70, 73, and 82, and the following not classified subtypes 42, 44, 54, 61, 62, 72, 81, 84, 90, and 91. The SPF10 primer set amplifies a 65 bp region in the L1 open reading frame of the HPV genome. DNA was extracted on a Maxwell, MDx Research System (Promega, Fitchburg, WI). The CHIPRON system includes internal hybridization controls and additional beta-globin spots to ascertain amplificability of extracted DNA as well as absence of polymerase chain reaction inhibitors. All assays were performed alongside a known positive and a known negative sample. All lesions were stained with antibody to p63 as marker of squamous differentiation, antibody to $p16^{ink4a}$ as surrogate marker for transforming HPV infections, and antibodies to p53, CK7, and CK17.

A superficial biopsy of the HPV-negative well-differentiated SCC of patient #7 was initially misdiagnosed as extensive HSIL only at an outside institution which resulted in imiquimod treatment for several months. Only repeat biopsies and conization for persistent disease 1 year later allowed correct diagnosis and revision of initial diagnosis. This erroneously diagnosed HSIL is 1 of the 2 HPV-negative precursor lesions reported previously in Reich et al.[10]

Mutational Analysis

Next-generation sequencing (NGS) libraries for mutational screening were prepared using the AmpliSeq library kit 2.0 (Thermo Fisher Scientific) and the Ion Ampliseq Cancer Hotspot Panel V2 (Cat Nr: 4475346) primer pool covering hotspot mutations in 50 genes implicated in cancer. Sequencing was done on an Ion S5XL benchtop sequencer (Thermo Fisher Scientific) to a length of 200 bp and initial data were analyzed using the Ion Torrent Suite Software Plug-ins (Thermo Fisher Scientific, open source, GPL, https://github.com/iontorrent/). Briefly, this included base calling, alignment to the reference genome (HG19) using the TMAP mapper and variant calling by a modified diBayes approach taking into account the flow space information. The following genes were analyzed: ABL1, AKT1, ALK, APC, ATM, BRAF, CDH1, CDKN2A, CSF1R, CTNNB1, EGFR, ERBB2, ERBB4, EZH2, FBXW7, FGFR1, FGFR2, FGFR3, FLT3, GNA11, GNAQ, GNAS, HNF1A, HRAS, IDH1, IDH2, JAK2, JAK3, KDR, KIT, KRAS, MET, MLH1, MPL, NOTCH1, NPM1, NRAS, PDGFRA, PIK3CA, PTEN, PTPN11, RB1, RET, SMAD4, SMARCB1, SMO, SRC, STK11, TP53, and VHL. Proper polymerase chain reaction amplification of all amplicons and even distribution of NGS reads was documented in coverage analysis and plots of each sample. Called variants were annotated using open source software ANNOVAR[11] and SnpEff.[12] All coding, nonsynonymous mutations were further evaluated and visually inspected in IGV (www.broadinstitute.org/igv/) and variant calls resulting from technical read errors or sequence effects were excluded from the analysis. Germline variants were classified as "common genetic variants" with an allele frequency > 3%. in the 1000 Genomes Project database (Annovar 1000g2015aug dataset). All variants with a mutational allelic frequency (MAF) < 3% were classified as "rare genetic variants." ClinVar database entries were accessed and reviewed for all rare genetic variants (www.ncbi.nlm.nih.gov/clinvar/). Rare germline variants were additionally cross-checked in data from a control group of 160 patients with HPV-induced HSIL and invasive SCC from our archives.

Chromosomal copy number variations were determined by low-density whole-genome sequencing. Library preparation was performed using the NEBNext Fast DNA Library Prep Set for Ion Torrent (New England Biolabs) from 50 ng DNA according to manufacturer's recommendations, and sequencing was done on Ion Torrent S5XL to a depth of ~5 million reads per sample. Sequence data was aligned to the reference genome (hg19) and copy number variations were called using the bioconductor package CNAnorm.[13] In addition, all NGS reads from this library were processed using the PathSeq[14] pipeline of the GATK, version 4.1.0[15] to detect unknown pathogen and HPV genomic sequences.[16] Institutional review board approval was obtained on November 27, 2018 (31-049 ex 18/19).

RESULTS

The average age of the 9 patients was 47 years (range: 36 to 65 y). In all, 3/9 patients had an intraepithelial precursor lesion without associated invasive SCC (patient #1 to #3; Figs. 1, 2A–D), 1/9 patients had a pT1a1 invasive SCC (patient #4; Figs. 2E–H), and 5/9 women had a widely invasive SCC without metastases (patient #5 to #9; pT1b [n = 2], pT2a [n = 2], pT3b [n = 1], Figs. 3, 4). All lesions were negative for DNA of 32 HPV genotypes and mRNA of 14 HPV genotypes. Analysis of all NGS reads for the presence of pathogens revealed only known contaminants. Genomic HPV sequences were absent in all samples except for a single read from the E1 region of the HPV genome in the pT1a1 SCC (patient #4).

The intraepithelial lesions, the pT1a1 SCC and 1 pT1b SCC were diagnosed on abnormal cytology smears and biopsy, and treated with cone excisions. The main symptom of widely invasive SCC was bleeding. Definitive treatment of the 2 pT1b SCC was hysterectomy and lymphadenectomy; the remaining 4 patients underwent

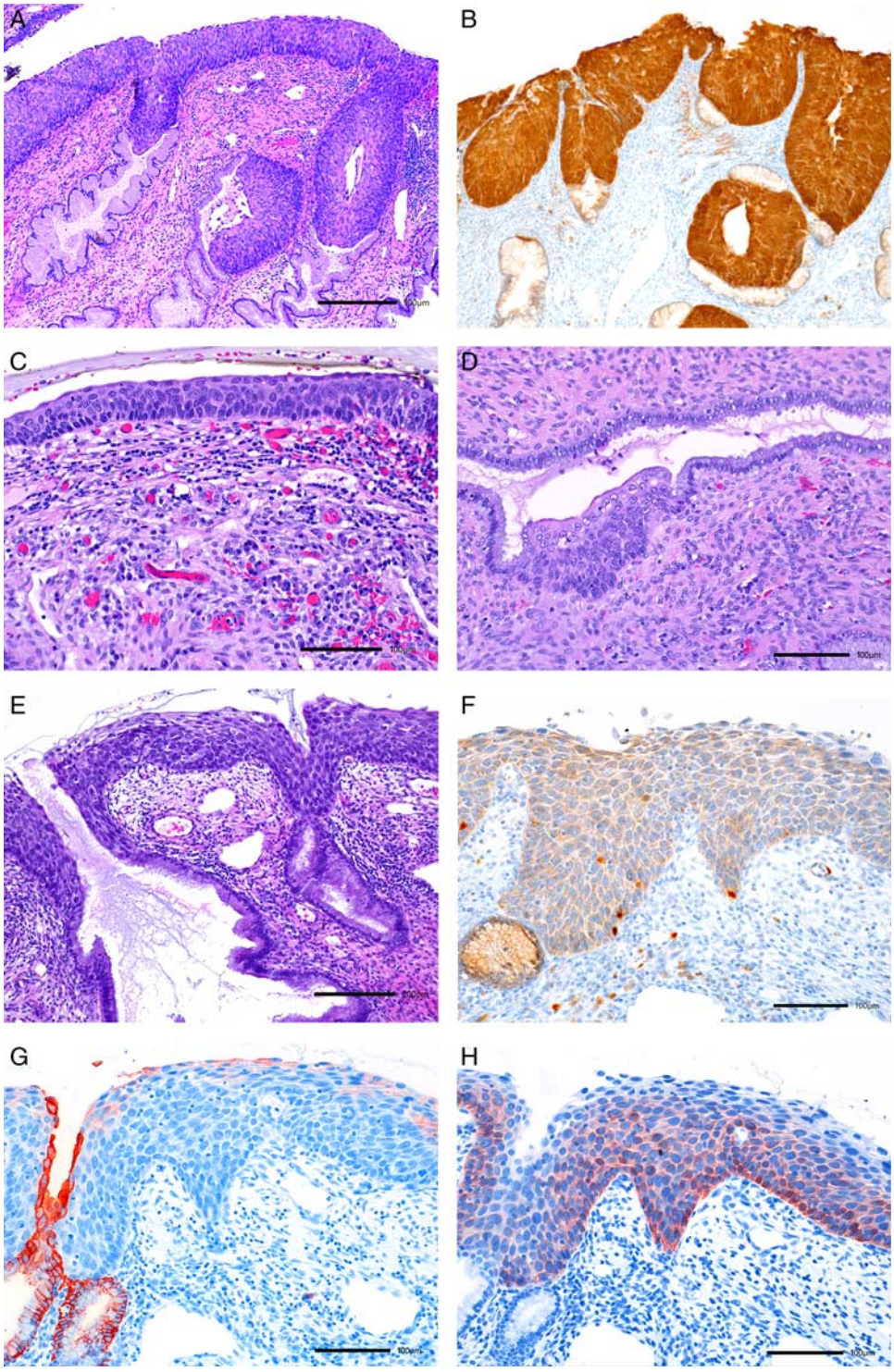

FIGURE 1. HPV-DNA and mRNA negative intraepithelial precursor lesions. *Patient #1*: A, HPV-negative precursor lesion without maturation or koilocytic changes of around 10 cell layers thickness involving the surface epithelium and the glands. B, Corresponding immunohistochemical stain with antibody to $p16^{ink4a}$ reveals block staining/$p16^{ink4a}$ overexpression. C, A different area of the HPV-negative precursor lesion resembling a thin HSIL with 5 cell layers thickness. D, A small early precursor lesion arises directly from reserve cells within a deeply located cervical gland. *Patient #2*: A precursor lesion of around 10 cell layers thickness extends along the surface (E) and shows no staining with antibody to $p16^{ink4a}$ (F). G, This HPV-negative precursor lesion is CK7 negative. Please note the strong staining of tall columnar endocervical cells. H, CK17 expression in the basal and suprabasal cell layers.

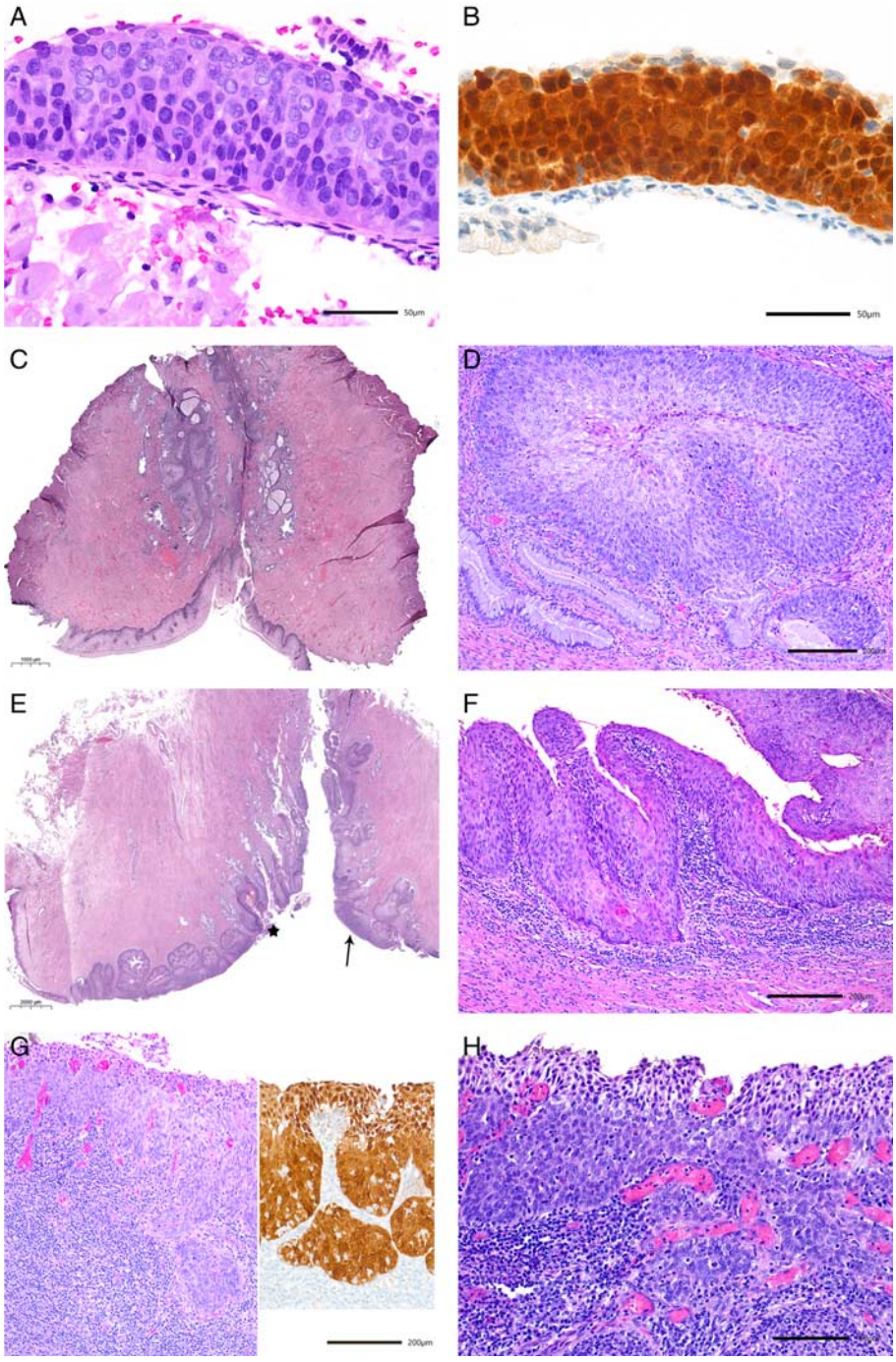

FIGURE 2. *Patient #3: HPV-DNA and mRNA negative intraepithelial precursor lesion.* A, The initial biopsy showed isolated strips of dysplasia involving the full thickness of the epithelium. The HPV-negative precursor lesion shows a uniform proliferation of basaloid keratinocytes with loss of polarity, no maturation or koilocytic changes, and an occasional mitosis. B, Immunohistochemical block staining of all cells including the basal cells with antibody to $p16^{ink4a}$. C, The full extent of the precursor lesion becomes evident in the cone specimen. There is extensive gland involvement high up in the endocervical canal. Also note that the intraepithelial precursor lesions extend along glands deep into the stroma. D, High power view of the intraglandular squamous precursor lesion. *Patient #4: pT1a1 SCC, HPV-DNA and mRNA negative, single HPV16 NGS read (E1).* E, The cone specimen of the pT1a1 SCC shows (similar to C) an extensive involvement of glands with a sharp transition from stratified squamous epithelium to in situ lesion. * indicates high power view in (F) and →indicates high power view in (G). F, An area of superficial invasion with keratinizing histology (indicated with * in E), accompanied by a lymphohistiocytic inflammatory infiltrate. G, An area of superficial invasion featuring basaloid histology (indicated with → in E), accompanied by a dense lymphohistiocytic inflammatory infiltrate, shows $p16^{ink4a}$ staining. H, The invasive basaloid SCC features numerous microvessels in the tumor stroma.

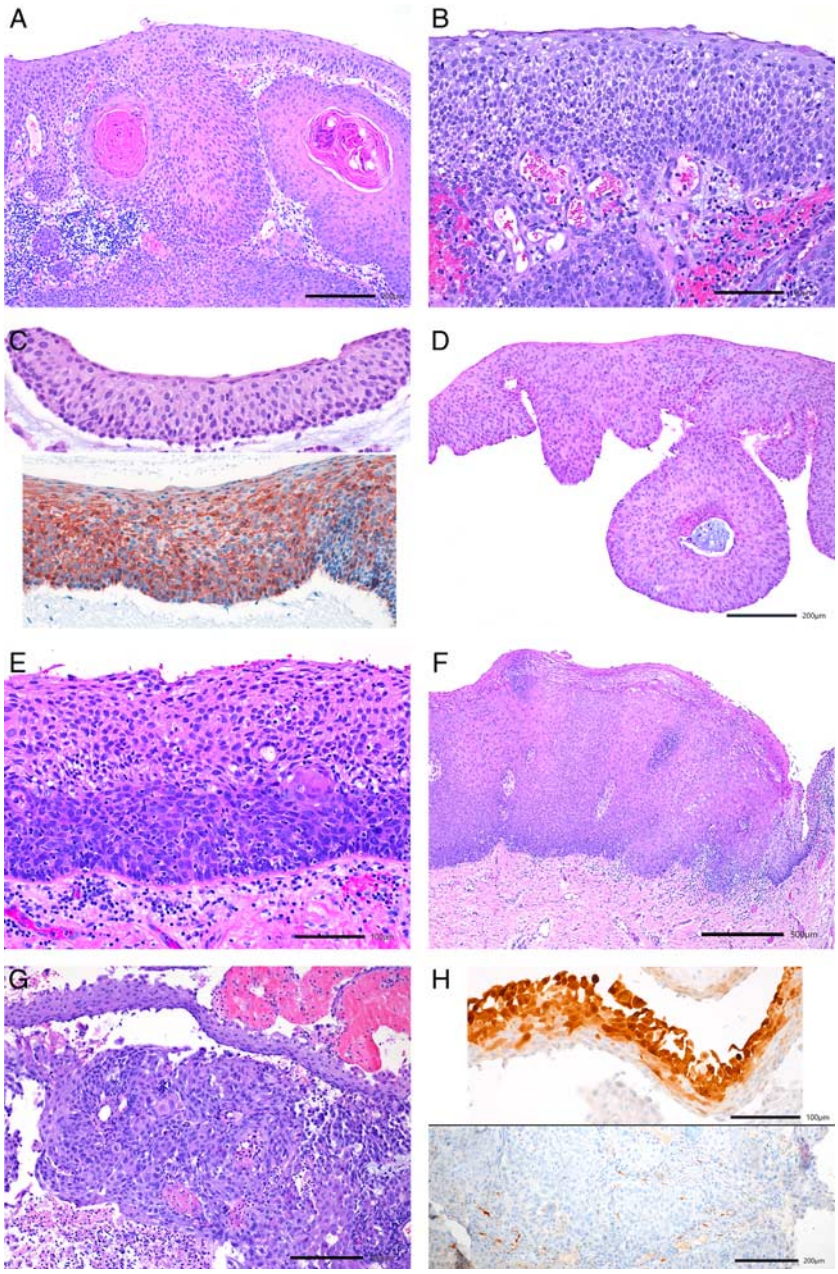

FIGURE 3. *Patient #6: pT2a SCC with GNAS mutation; dead of disease*. A, A bland inconspicuous in situ component overlies a highly keratinized SCC. B, Other preinvasive areas were >10 cell layers thick bland undifferentiated proliferations with extensive intraepithelial edema, and prominent subepithelial blood vessels. *Patient #7*: SCC with 4 different specimens; PIK3CA and STK11 mutations, dead of disease. C, The initial biopsy contained small, isolated, CK17-positive strips of full-thickness precursor lesion <9 cell layers thick. D, Admixed with large fragments of highly differentiated, keratinized intraepithelial proliferation. E, The cone specimen obtained 1 year after the first biopsy and after several months of Imiquimod therapy revealed an extensive full-thickness intraepithelial proliferation. There was a basaloid proliferation in lower cell layers contrasting the abortive maturation in the superficial half to the epithelium and premature squamatization featuring a keratin pearl in the mid-portion with ample pink cytoplasma of the preinvasive lesion. F, In other areas, the intraepithelial lesions were extremely thick with a predominant highly atypical basal and suprabasal proliferation, with largely maintained "normal" superficial maturation featuring parakeratosis. Note the sharp transition/border between nontumorous, atrophic squamous epithelium and the in situ carcinoma. *Patient #8*: pT3b SCC. G, Biopsy material of a partly keratinizing SCC with isolated strips of flat bland and atrophic appearing squamous intraepithelial in situ component with hemorrhage. H, The invasive SCC shows no $p16^{ink4a}$ staining. The isolated strips of intraepithelial proliferations showed patchy heterogenous $p16^{ink4a}$ staining in the superficial cell layers with sparing of basal cells. This staining does not represent overexpression.

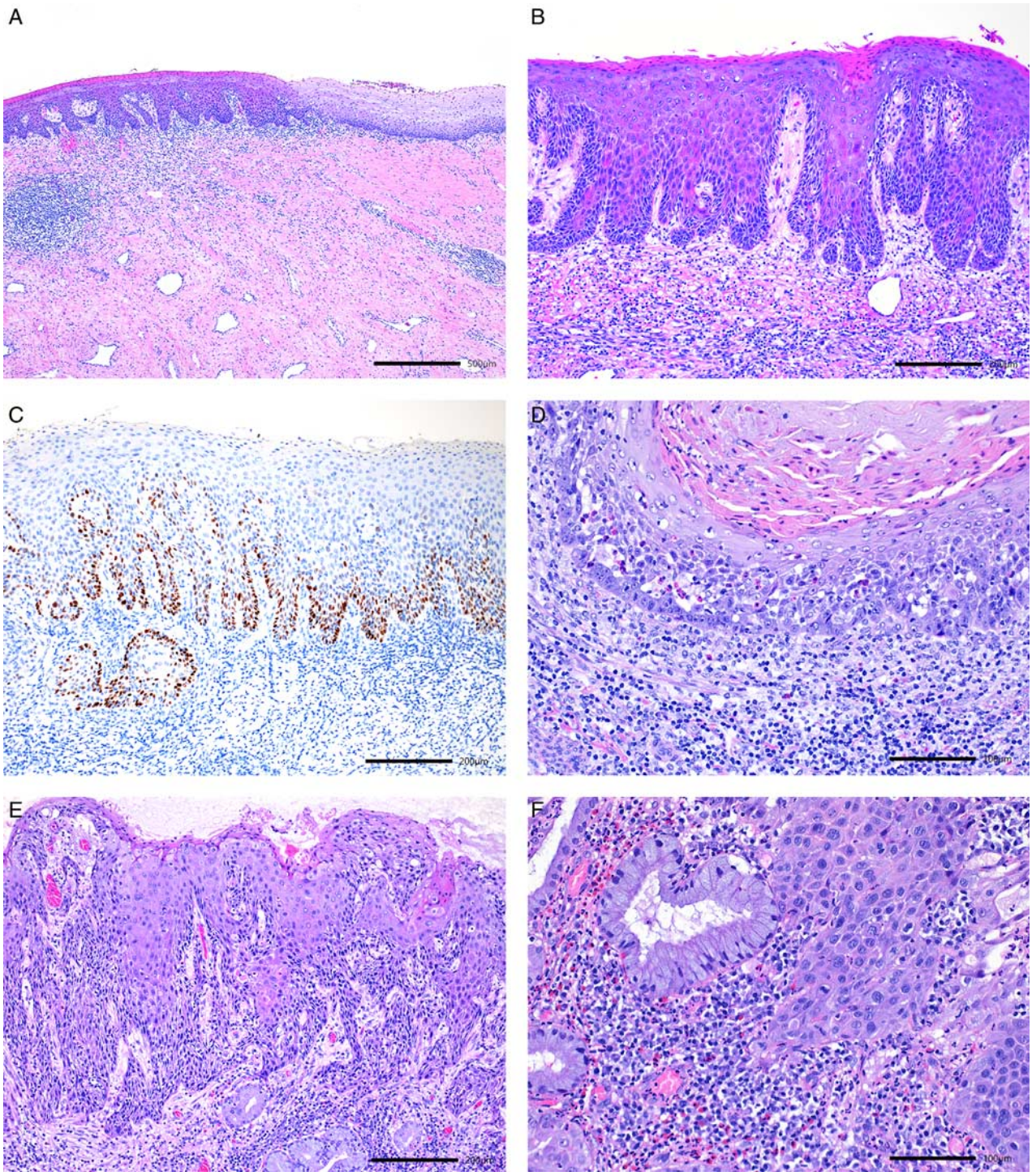

FIGURE 4. Keratinized precursor lesions/in situ components. *Patient #9*: pT1b SCC with *TP53* gene mutation (likely pathogenic missense mutation). A, There is a sharp and abrupt transition between nontumorous glycogenated squamous epithelium and intraepithelial precancerous lesion. B, The basal and suprabasal proliferation has a high mitotic index. Premature squamatization with large cells with ample pink cytoplasm in suprabasal cell layers is prominent. Parakeratosis is present. This histology is reminiscent of differentiated vulvar intraepithelial neoplasia. C, Nuclear p53 staining in basal and suprabasal keratinocytes of precursor lesion and invasive SCC. D, The invasive SCC and stroma were densely infiltrated by eosinophilic granulocytes. *Patient #5*: pT1b SCC. E, The in situ component of the partly keratinizing pT1b SCC showed a proliferation of basal and suprabasal cells with partly premature squamatization and superficial squamous maturation with focal parakeratosis. F, The invasive SCC features numerous eosinophilic granulocytes in the peritumoral stroma.

staging lymphadenectomies and received standard chemoradiation therapy. Two patients progressed despite chemoradiation therapy and died of extensive local pelvic/abdominal disease within 24 and 36 months after initial diagnosis, but they had no lymphatic or hematogenous metastases (Table 1).

INTRAEPITHELIAL PRECURSOR LESIONS WITHOUT INVASIVE SCC

Primary diagnoses were made on biopsy specimens, but the full extent of the precursor lesions was appreciated only in the cone specimens. The HPV-negative precursor lesions occurred throughout the entire transformation zone, partly deep inside the endocervical canal. The precursor lesions involved the surface epithelium (Figs. 1A–D), but also extended deep into the cervical glands (Figs. 1A–C, patient #1; Figs. 1D–F, patient #2), partly inside the endocervical canal (Figs. 1D, 2C; patient #3). Epithelial thickness ranged from 3 to 20 cell layers, but was typically around 10 cell layers (Figs. 1A–H, 2A). The undifferentiated proliferation with loss of polarity, nuclear atypia and numerous mitoses was indistinguishable from HPV-associated basaloid HSIL on conventional HE-histology. All precursor lesions showed nuclear p63 expression. One precursor lesion was CK7 negative (Fig. 1G), an inhomogeneous focal CK7 and CK17 staining was observed in 2/3 precursor lesions (Fig. 1H). In all, 2/3 HPV-negative intraepithelial lesions revealed a homogenous diffuse $p16^{ink4a}$ block staining in all dysplastic cells including basal keratinocytes, indistinguishable from $p16^{ink4a}$ overexpression in HPV-induced HSIL (Figs. 1B, 2B). Nuclear p53 staining of individual basal nuclei corresponded to wild-type p53 protein. Somatic gene mutations in hotspot regions of 50 cancer genes were absent, but 1/3 precursor lesions had a gain of chromosome 3q.

INVASIVE KERATINIZING SCC

Superficially Invasive SCC

The pT1a1 SCC (Figs. 2E–H; patient #4) was the only case which demonstrated a single read of HPV16 E1 DNA after of HPV sequencing. It arose in an extensive, p63-positive, CK7-negative intraepithelial lesion $\geq$10 cell layers thick with $p16^{ink4a}$ block staining that involved predominantly endocervical glands (Fig. 2E). Multiple foci of invasion were identified; some were keratinized (Fig. 2F), but the majority revealed basaloid histology (Fig. 2G). The stroma had a dense lymphocyte-dominated inflammatory infiltrate with plasma cells and occasional stromal eosinophilic granulocytes. The stroma was highly vascularized with numerous small blood vessels, particularly around the basaloid invasive foci (Fig. 2H). Somatic gene mutations in hotspot regions of the analyzed 50 genes were absent, but gains of chromosome 3q were present.

Invasive Keratinizing SCC $\geq$ pT1b

All 5 widely invasive HPV-negative keratinizing SCC were diagnosed on biopsy material. The extensive invasion, however, was not appreciated in 2 patients, who underwent cone excisions before definitive treatment. For the remaining 3 SCC, biopsy material only was available for analysis (Fig. 2C, patient #5; Fig. 2D, patient #6). All invasive cancer components were p63-positive and $p16^{ink4a}$-negative keratinizing SCC without glandular differentiation. The dense inflammatory infiltrate featured lymphocytes and plasma cells, and in 3/5 SCC numerous stromal and/or intratumoral eosinophilic granulocytes. Numerous subepithelial microvessel were present in the stroma of 4/5 SCC. In situ components were observed in all invasive SCC. In diagnostic biopsies they were present occasionally as isolated strips admixed with fragments of invasive SCC (Figs. 2A, B, 3C, D, 3G, D, H). In cone excisions, a sharp and abrupt transition between nonsquamous glycogenated epithelium and intraepithelial cancer was observed (Fig. 4A). In situ components/precursor lesions showed heterogenous histology. The majority were full-thickness basaloid intraepithelial proliferations with loss of polarization, nuclear atypia, and mitotic activity with an epithelial thickness between 5 and 10 cell layers. Occasionally, the in situ component appeared flat and atrophic. Other precursor lesions (Figs. 3C–F, 4A–F) were highly differentiated and keratinizing, and resembled the HPV-negative precursor lesion in vulva, the differentiated intraepithelial neoplasia. They featured an atypical proliferation of basal and suprabasal keratinocytes, numerous mitoses, and premature squamatization. Superficial squamous maturation was largely maintained but featured parakeratosis and hyperkeratosis (Fig. 4). The in situ components—with the exception the *TP53* gene mutated SCC with nuclear p53 overexpression—revealed "wild-type" p53 staining. Inconsistent CK7 staining was observed in 1/5 SCC, and CK17 expression in 3/5 SCC. Only 1/5 invasive SCC showed inhomogeneous $p16^{ink4a}$ staining in the in situ component in superficial cell layers only with sparing of the basal cell layers (Fig. 3H, patient #8).

Genetic Aberrations

Somatic gene mutations were identified in 3/6 widely invasive SCC (2 pT1b SCC and 1 pT2a SCC). One SCC (patient #9) revealed concomitant somatic mutations in the *TP53* gene (G154S; uncertain significance) and the SMARCB2 gene (R377H; likely pathogenic). The second SCC (patient #5) with 2 biopsies obtained within 3 weeks revealed identical mutations in the GNAS gene (S848C; likely pathogenic). The third SCC (patient #7) with 4 biopsies featured inconsistent PIK3CA gene mutations at low allelic frequency in the hotspot location E545K in the initial biopsy, and in the hotspot location E542K in 1/3 follow-up biopsies with a concomitant mutation in the STK11 gene. Two patients with the somatic gene mutations died due to complications of extensive pelvic disease without lymphatic or hematogenous metastases. Three

TABLE 1. HPV-negative Precursor Lesions and Invasive SCC

Patient #	Age at Diagnosis (y)	Diagnosis at 1° Present-ation	Histology	HPV Reads in NGS	$p16^{ink4a}$	p53	Somatic Gene Mutations	Germline polymorphisms	Copy Number Variations	Follow-up	Figures
1	36	Precursor lesion	Mostly thick precursor lesion > 10 cell layers, adjacent to thin lesions 3-5 cell layers thick; involving surface and glands opening	0/ 8045213	Positive	WT	None	Heterozygote: PIK3CA: NM_006218: exon7:c.A1173G: p.I391M Heterozygote: KIT: NM_000222: exon10:c. A1621C:p. M541L Homozygote: KDR: NM_002253: exon11:c. A1416T:p.Q472H Heterozygote: TP53: NM_000546: exon4:c.C215G:p. P72R	Gain 1p21.2-36.31 Gain 3q	Alive 54 mo	Figs. 1A–D
2	41	Precursor lesion	5-9 cell layers thick; predominatly on the surface epithelium; pseudokoilocy-tosis; dense inflammation	0/ 8556339	Negative	WT	None	Homozygote: TP53: NM_000546: exon4:c.C215G:p. P72R	None	Alive 46 mo	Figs. 1E–H
3	42	Precursor lesion*	> 10 cell layers; extensive gland involvement; scant in-flammatory infiltrate	0/ 7279989	Positive	WT	None	Heterozygote: KIT: NM_000222: exon10:c. A1621C:p. M541L Heterozygote: KDR: NM_002253: exon11:c. A1416T:p.Q472H Heterozygote: APC: NM_000038: exon16:c. C4073T:p. A1358V* Heterozygote: TP53: NM_000546: exon4:c.C215G:p. P72R	None	Alive 109 mo	Figs. 2A–D
4	36	SCC pT1a1; conization	*Invasive SCC*: Keratinizing and basaloid, highly vascularized stroma, dense lymphocyte predominant inflammation *In situ component*: Mostly basaloid	1/ 2339548	Positive	WT	None	Heterozygote: KDR: NM_002253: exon11:c. A1416T:p.Q472H Homozygote: TP53: NM_000546: exon4:c.C215G:p. P72R Heterozygote: JAK3: NM_000215: exon16:c. G2164A:p.V722I	Gain 3q Loss 13	Alive 105 mo	Figs. 4E, F

TABLE 1. (*continued*)

Patient #	Age at Diagnosis (y)	Diagnosis at 1° Presentation	Histology	HPV Reads in NGS	p16^{ink4a}	p53	Somatic Gene Mutations	Germline polymorphisms	Copy Number Variations	Follow-up	Figures
5	41	SCCpT1-b1; pN0; biopsy	*Invasive SCC*: Keratinizing, highly vascularized, dense inflammation with plasma cells and eosinophilic granulocytes *In situ component*: Reminiscent of d-VIN	0/4068826	Negative	WT	None	Heterozygote: KDR: NM_002253: exon11:c.A1416T:p.Q472H Homozygote: TP53: NM_000546: exon4:c.C215G:p.P72R	None	Alive 49 mo	Figs. 2A–D
6	46	SCC pT2a; pN0; 2 different biopsies	*Invasive SCC*: Keratinizing; highly vascularized; dense inflammation; intratumoral and stromal eosinophilic granulocytes *In situ lesion*: Undifferentiated, spongiotic	0/3917528	Negative	WT	*GNAS*: NM_000516: exon8:c.C614G:p.S205C; MAF 25%	Heterozygote: KDR: NM_002253: exon11:c.A1416T:p.Q472H Heterozygote: TP53: NM_000546: exon4:c.C215G:p.P72R	Gain 9 Loss 19p	DOD 24 mo	Figs. 3A, B
7	57	Invasive SCC† with in situ component; biopsy; 2017	*Invasive SCC*: Well-differentiated, keratinizing *In situ component*: Basaloid and keratinizing SCC in situ	0/3943267	Negative	WT	*PIK3CA*: NM_006218: exon10:c.G1633A:p.E545K; MAF 5%†	Homozygote: TP53: NM_000546: exon4:c.C215G:p.P72R	Gain 3q Loss 4p15.2-16.3 Gain 10p12.31-15.3	DOD 36 mo	Figs. 3C–F
		SCC pT2a; pN0; conization; 2018	*Invasive SCC*: Mostly basaloid in glands; with predominant *In situ component*: basaloid and keratinizing	0/9090654	Negative	WT	*PIK3CA*: NM_006218: exon 10: c.G1624A:p.E542K; MAF17% *STK11*: NM_000455: exon1: c.G97C:p.E33Q MAF 11%	Homozygote: TP53: NM_000546: exon4:c.C215G:p.P72R	Gain 3q		
		SCC pT2a; pN0: 2 separate biopsies, 1 before and 1 after conization	*Invasive SCC*: Partially keratinizing; highly vascularized stroma, dense inflammation with stromal eosinophilc granulocytes *In situ component*: Partly basaloid, partly keratinizing	0/13381574	Negative	WT	None	Homozygote: TP53: NM_000546: exon4:c.C215G:p.P72R	Gain 3q Loss 4p15.2-16.3 Gain 10p13-15.35		
8	60	Pre-invasive component of pT3b SCC; pN0; biopsy	Thin atrophic 5 cell layers thick, analyzed separately from invasive component	0/7364806	Positive	WT	None	Heterozygote: KDR: NM_002253: exon11:c.A1416T:p.Q472H Homozygote: TP53: NM_000546:exon4:c.C215G:p.P72R	Gain 3q22.1-29 Gain 8q Gain 22	Alive 14 mo	Figs. 3G, H

TABLE 1. (*continued*)

Patient #	Age at Diagnosis (y)	Diagnosis at 1° Present-ation	Histology	HPV Reads in NGS	$p16^{ink4a}$	p53	Somatic Gene Mutations	Germline polymorphisms	Copy Number Variations	Follow-up	Figures
		Invasive component SCC pT3b; biopsy	Partly keratinizing, well-vascularized stroma, scant inflammation	0/3758039	Negative	WT	None	Heterozygote: KDR: NM_002253: exon11:c. A1416T:p. Q472H Homozygote: TP53: NM_000546: exon4:c. C215G:p.P72R	Gain 3q22.1-29 Gain 8q Gain 22		Figs. 3G, H
9	65	SCC pT1b; pN0; biopsy	*Invasive SCC*: Well-differentiated, keratinizing dense inflammation with intratumoral and stromal eosinophilic granulocytes *In situ component*: Reminiscent of d-VIN	0/4307023	Negative	Nuclear p53 overexpression	*TP53*: NM_000546: exon 5, G145S; MAF 10% *SMARCB1*: NM_003073: exon 9, R377H; MAF 5%	Heterozygote: Notch: NM_017617: exon 34: T2466M Heterozygote: KDR: NM_002253: exon11:c. A1416T:p. Q472H Heterozygote: TP53: NM_000546: exon4:c. C215G:p.P72R	None	Alive 2 mo	Figs. 4A–D

*Previously reported in Reich et al.[10]
†Previously reported as HSIL in Reich et al.[10]
1° indicates primary; DOD, indicates dead of disease; d-VIN, differentiated vulvar intraepithelial neoplasia; WT, "wild-type" staining of p53.

SCC were devoid of somatic gene mutations, but 2 of these 3 SCC featured complex chromosomal copy number variations.

GERMLINE VARIANTS IN PREINVASIVE LESIONS AND INVASIVE SCC

All patients carried possibly pathogenic germline variants in 1 to up to 4 different genes. The common germline variants in the TP53, KDR, and KIT genes occurred at higher percentages in our patient cohort when compared with the general population according to the dbSNP (www.1000genomes.org). The germline variant P72R in the *TP53* gene was present in all patients with an overall MAF of 72% (4 homozygous, 5 heterozygous patients) compared with 54% in the general population. The pathogenic Q472H polymorphism in the kinase insert domain receptor (KDR) gene, which is encoded by vascular endothelial growth factor (VEGF) 2, occurred in 7/9 (78%) women. The MAF of 50% (1 patient with homozygous and 6 patients with heterozygous polymorphisms) was higher than the 21% in the control group of HPV-induced HSIL/invasive SCC and the 21% in the general population (please note the wide range of this germline variation in the general population: 9% in African American; 13% in white Americans; 47% in Asian populations; details see 1000Genomes Project database; www.1000genomes.org). The M541L variant in the KIT gene with was detected in 2/3 patients with preinvasive lesions with a MAF of 12.5% versus 6.45% in the general population. Rare germline variants were detected in the JAK3 gene (V722I) in the patient with the pT1a1 SCC (MAF of 6% vs. 0.36%) and in the APC gene in the previously reported patient with a preinvasive lesion. Patient #9 carried a NOTCH variant (T2466M) which is likely benign and described with very low frequency in healthy adults (8/98176 alleles in the genomAD database of the European [non-Finnish] population).

DISCUSSION

In 2020 the WHO officially acknowledged the existence of HPV-independent invasive cervical SCC. HPV-independent precursor lesions, however, were not included, since none had been described yet. In this paper, we present a detailed first description of HPV-negative high-grade cervical precursor lesions without invasive SCC. HPV-negativity was defined as lack of both, DNA of 32 HPV subtypes and E6/E7 mRNA of 14 HPV subtypes, and additionally by the absence of HPV sequences in WGS reads.[16] Our cases are thus different from HPV-

independent SCC that contained HPV-DNA but did not express HPV transcripts.[17] All lesions in this study arose within the metaplastic squamous epithelium of the transformation zone with an abrupt transition between precursor lesion and squamous epithelium of the exocervix. The majority resembled thick and thin HPV-induced HSIL as defined by the WHO,[18] but some cervical precursor lesions were highly keratinized proliferations akin to differentiated vulvar intraepithelial neoplasia . Some preinvasive HPV-negative lesions featured diffuse block staining/overexpression of $p16^{ink4a}$, reminiscent of transforming HPV-infection after HPV-E7 oncogene-induced inactivation of the retinoblastoma (Rb) protein pathways. The keratinized HPV-negative invasive SCC showed a strikingly vascularized stroma with a dense inflammatory infiltrate, partly with numerous stromal and intratumoral eosinophilic granulocytes. All invasive SCC lacked $p16^{ink4a}$ staining, contrasting reports about $p16^{ink4a}$ block staining of the invasive components in 8/12 HPV-independent SCC.[7] $p16^{ink4a}$ block staining in our study was unrelated to somatic gene mutations or germline polymorphisms in the Rb gene, or the CDKN2A gene on chromosome 9p21.3, which encodes for $p16^{ink4a}$. A disrupted $p16^{ink4a}$-CDK4/6-Rb axis is a common pathway of numerous cancers. Defective Rb-signaling and G1/S checkpoint regulation[19] may be related to chromosomal copy number variations (eg, loss of chromosome 13, or gain of chromosome 9) or hypermethylation of the $p16^{ink4a}$ promoter[20] and the CDKN2A gene. Other explanations for aberrantly elevated $p16^{ink4a}$ include production of an abnormal Rb protein as shown in a HPV-negative cervical cancer cell line,[21] or cellular reaction to DNA damage, production of oxygen species, telomere erosion, stalled replication forks (for review, see the study by Burd et al[22]). Cellular stress during tissue injury may also account for occasional patchy and heterogenous $p16^{ink4a}$ staining.

In contrast to HPV-induced cervical SCC,[23,24] consistent activating somatic gene mutations appear irrelevant in HPV-negative squamous cervical carcinogenesis. Low allelic frequency of gene mutations indicates tumor heterogeneity. Activating GNAS gene mutations are common in invasive mucinous cervical adenocarcinomas[23] and glandular endocervical hyperplasia,[25] but are exceptionally rare in HPV-induced cervical SCC and absent in HPV-negative SCC. Similarly, tumor suppressor gene mutations appear irrelevant in the development of HPV-negative cervical SCC. *TP53* gene mutations reported in HPV-negative cervical cell lines[21] likely were owed to karyological instability due to continued passages of cultured cells. Chromosomal aberration, however, can substitute for gene mutations,[26–28] similar to HPV-induced carcinogenesis, where gains of 3q with subsequent activation of TERC and PIK3 pathways are considered early events in carcinogenesis.[29,30]

Due to the small number of HPV-negative cervical precancers and invasive SCC in our study and in general, many unanswered questions remain with respect to the cellular origin and triggers for initial abnormal proliferation, as well as the natural course of HPV-negative SCC including drivers of progression. The contribution of the inflammatory infiltrate to HPV-negative squamous carcinogenesis needs further investigation. Particularly eosinophilic granulocytes have been linked to unfavorable prognosis,[31,32] probably due to their role in tumor angiogenesis via VEGF production.[33] The pathogenic germline variant Q472H in the KDR gene can also enhance proliferation, migration and sprouting of tumoral endothelial cells via increased VEGF-2 receptor phosphorylation and VEGF secretion. This angiogenic germline variant conferred significantly higher tumor microvessel densities and higher serum VEGF levels in melanoma patients[34] possibly making these patients eligible for anti-angiogenesis treatment such as targeted VEGF receptor 2 inhibition. Progressive local pelvic and abdominal disease, however, may be the result of a growth advantage of small tumor cell clones with activating somatic gene mutations or chromosomal aberrations.

We demonstrate in this paper for the first time, that HPV-negative cervical precursor lesions exist. All HPV-negative invasive cervical SCC had clearly identifiable intraepithelial precursors, either highly differentiated and keratinized proliferations reminiscent of differentiated vulvar intraepithelial neoplasia, or undifferentiated basaloid proliferations reminiscent of HSIL with occasional diffuse block staining of $p16^{ink4a}$. Finding an appropriate new terminology for these extremely rare HPV-negative precursor lesions, however, proves difficult. They are not classifiable according to the Lower Anogenital Squamous Terminology (LAST) Standardization Project for HPV-Associated Lesions.[35] In analogy to terminology of vulvar carcinogenesis, HPV-independent or differentiated cervical intraepithelial neoplasia may be an appropriate nomenclature.

It is unclear at this moment, what implications, if any, result from missing one of these rare cases in routine surgical pathology. Lack of information on the natural course of HPV-negative precursor lesions and SCC, and the lack of specific therapy options do not warrant automatic HPV genotyping on basaloid $p16^{ink4a}$ overexpressing cervical intraepithelial proliferations. Further workup may be indicated, however, for the readily recognizable highly differentiated intraepithelial precursor lesions or keratinizing SCC, as presence of mutations in tumor suppressor genes may render these SCC less sensitive to chemoradiation therapy. Overall, the oncogenic triggers remain elusive, but dense inflammatory infiltrates and the pathogenic germline variant Q472H in the KDR gene may contribute to tumor angiogenesis and progression of HPV-negative cervical carcinogenesis.

REFERENCES

1. zur Hausen H. Papillomaviruses and cancer: from basic studies to clinical application. *Nat Rev Cancer*. 2002;2:342–350.
2. Halec G, Alemany L, Lloveras B, et al. Pathogenic role of the eight probablly/possibly carcinogenic HPV types 26, 53, 66, 67, 68, 70, 73 and 82 in cervical cancer. *J Pathol*. 2014;234:441–451.
3. Snijders PJF, Steenbergen RDM, Heideman DAM, et al. HPV-mediated cervical carcinogenesis: concepts and clinical implications. *J Pathol*. 2006;208:152–164.
4. Tuna M, Amos CI. Next generation sequencing and its applications in HPV-associated cancers. *Oncotarget*. 2017;8:8877–8889.

5. Sacco A, Carrilho C, Focchi GRS, et al. Tumours of the uterine cervix. *WHO Classification of Tumours Female Genital Tumors*. Lyon, France: IARC; 2020:350–351.
6. Kaliff M, Karlsson MG, Sorbe B, et al. HPV-negative tumors in a swedish cohort of cervical cancer. *Int J Gynecol Pathol*. 2020;39: 279–288.
7. Nicolas I, Marimon L, Barnadas E, et al. HPV-negative tumors of the uterine cervix. *Mod Pathol*. 2019;32:1189–1196.
8. Bohmer G, van den Brule AJ, Brummer O, et al. No confirmed case of human papillomavirus DNA-negative cervical intraepithelial neoplasia grade 3 or invasive primary cancer of the uterine cervix among 511 patients. *Am J Obstet Gynecol*. 2003;189:118–120.
9. Petry KU, Cox JT, Johnson K, et al. Evaluating HPV-negative CIN2 + in the ATHENA Trial. *Int J Cancer*. 2016;138:2932–2939.
10. Reich O, Regauer S, Kashofer K. Possibly carcinogenic HPV subtypes are a cause of HSIL and negative clinical HPV tests—a European prospective single center study. *Gynecol Oncol*. 2020;158:112–116.
11. Wang K, Li M, Hakonarson H. ANNOVAR: functional annotation of genetic variants from high-throughput sequencing data. *Nucleic Acids Res*. 2010;38:e164.
12. Cingolani P, Platts A, Wang L, et al. A program for annotating and predicting the effects of single nucleotide polymorphisms, SnpEff: SNPs in the genome of *Drosophila melanogaster* strain w1118; iso-2; iso-3. *Fly (Austin)*. 2012;6:80–92.
13. Gusnanto A, Wood HM, Pawitan Y, et al. Correcting for cancer genome size and tumour cell content enables better estimation of copy number alterations from next-generation sequence data. *Bioinformatics*. 2012;28:40–47.
14. Kostic AD, Ojesina AI, Pedamallu CS, et al. PathSeq: software to identify or discover microbes by deep sequencing of human tissue. *Nat Biotechnol*. 2011;29:393–396.
15. McKenna A, Hanna M, Banks E, et al. The Genome Analysis Toolkit: a MapReduce framework for analyzing next-generation DNA sequencing data. *Genome Res*. 2010;20:1297–1303.
16. Arroyo Muhr LS, Lagheden C, Lei J, et al. Deep sequencing detects human papillomavirus (HPV) in cervical cancers negative for HPV by PCR. *Br J Cancer*. 2020;123:1790–1795.
17. Banister CE, Liu C, Pirisi L, et al. Identification and characterization of HPV-independent cervical cancers. *Oncotarget*. 2017;8:13375–13386.
18. Mills AM, Carhillo C, Focchi GRA, et al. Squamous intraepithelial lesions of the uterine cervix. *WHO Classification of Tumours Female Genital Tumors*. Lyon, France: IARC; 2020:342–346.
19. LaPak KM, Burd CE. The molecular balancing act of p16(INK4a) in cancer and aging. *Mol Cancer Res*. 2014;12:167–183.
20. Han YD, Wang XB, Cui NH, et al. Associations of P16INK4a promoter hypermethylation with squamous intra-epithelial lesion, cervical cancer and their clinicopathological features: a meta-analysis. *Oncotarget*. 2017;8:1871–1883.
21. Kalu NN, Mazumdar T, Peng S, et al. Genomic characterization of human papillomavirus-positive and -negative human squamous cell cancer cell lines. *Oncotarget*. 2017;8:86369–86383.
22. Burd CE, Sorrentino JA, Clark KS, et al. Monitoring tumorigenesis and senescence in vivo with a p16(INK4a)-luciferase model. *Cell*. 2013;152:340–351.
23. Zammataro L, Lopez S, Bellone S, et al. Whole-exome sequencing of cervical carcinomas identifies activating ERBB2 and PIK3CA mutations as targets for combination therapy. *Proc Natl Acad Sci USA*. 2019;116:22730–22736.
24. Martell K, McIntyre JB, Kornaga EN, et al. PIK3CA mutation and CNV status and post-chemoradiotherapy survival in patients with cervical cancer. *Gynecol Oncol*. 2020;158:776–784.
25. Matsubara A, Sekine S, Ogawa R, et al. Lobular endocervical glandular hyperplasia is a neoplastic entity with frequent activating GNAS mutations. *Am J Surg Pathol*. 2014;38:370–376.
26. Mitsuhashi A, Tanaka H, Tanaka N, et al. Establishment and characterization of a new HPV-negative squamous cell carcinoma cell line (Yumoto) from the human uterine cervix. *Gynecol Oncol*. 1998;70:339–347.
27. Allen DG, White DJ, Hutchins AM, et al. Progressive genetic aberrations detected by comparative genomic hybridization in squamous cell cervical cancer. *Br J Cancer*. 2000;83:1659–1663.
28. Verlaat W, Snijders PJF, Novianti PW, et al. Genome-wide DNA methylation profiling reveals methylation markers associated with 3q gain for detection of cervical precancer and cancer. *Clin Cancer Res*. 2017;23:3813–3822.
29. Snijders PJ, van Duin M, Walboomers JM, et al. Telomerase activity exclusively in cervical carcinomas and a subset of cervical intra-epithelial neoplasia grade III lesions: strong association with elevated messenger RNA levels of its catalytic subunit and high-risk human papillomavirus DNA. *Cancer Res*. 1998;58:3812–3818.
30. Hopman AH, Theelen W, Hommelberg PP, et al. Genomic integration of oncogenic HPV and gain of the human telomerase gene TERC at 3q26 are strongly associated events in the progression of uterine cervical dysplasia to invasive cancer. *J Pathol*. 2006;210: 412–419.
31. van Driel WJ, Hogendoorn PC, Jansen FW, et al. Tumor-associated eosinophilic infiltrate of cervical cancer is indicative for a less effective immune response. *Hum Pathol*. 1996;27:904–911.
32. Xie F, Liu LB, Shang WQ, et al. The infiltration and functional regulation of eosinophils induced by TSLP promote the proliferation of cervical cancer cell. *Cancer Lett*. 2015;364:106–117.
33. Varricchi G, Galdiero MR, Loffredo S, et al. Eosinophils: the unsung heroes in cancer? *Oncoimmunology*. 2018;7:e1393134.
34. Silva IP, Salhi A, Giles KM, et al. Identification of a novel pathogenic germline KDR variant in melanoma. *Clin Cancer Res*. 2016;22:2377–2385.
35. Darragh TM, Colgan TJ, Cox JT, et al. The lower anogenital squamous terminology standardization project for hpv-associated lesions: background and consensus recommendations from the college of american pathologists and the american society for colposcopy and cervical pathology. *Arch Pathol Lab Med*. 2012;136:1266–1297.